ICREN-01/2012 December 15-16, 2012 Constantine, Algeria
First International Conference on Renewable Energies and Nanotechnology impact on Medicine and Ecology

Development of a Spherical Solar Collector with a cylindrical receiver

Khaled MAHDI[a,b], Nadir BELLEL[a], a*

[a]*Laboratory of physics energy, Department of physics, Mentouri University of Constantine, Algeria*

[b]*Hydrometeorology Institute of formation and research, Oran, Algeria*

Abstract

Solar energy can be used for substitution of the depleting fossil fuels in thermal applications and electricity generation through thermal route. For medium and high temperature applications, a system for collecting solar energy at high temperatures was developed and built in this research work. The system, built at the center of development of renewable energy of the Algiers, consists of a $2\theta_m = 60°$ included angle, R_0 = 0.90 m diameter spherical reflector with a cylindrical receiver filled with water, tracking reflector which moves into the focus following the sun's movement. The system is capable of heating water or other fluids to temperatures above 350°C, thus making it possible to obtain process heat for domestic use and to store solar energy in a compact and economical way. An analysis of the system's optical characteristics was performed to aid in the design of the spherical reflector and cylindrical receiver. The thermal performance of the system was analyzed. The effects of mirror reflection, concentration ratio, heat transfer to the fluid (water), incidence angle, size and form of the cylindrical receiver, environmental conditions (wind, ambient temperature), have been studied by means of thermal model.

The performance of the spherical reflector was tested by the temperature of the water. Total efficiencies (solar to thermal) of $\eta_{th} = 60\%$-70% were obtained for a wide range of temperatures up to 350°C. The results of the present study show that it is possible to use the spherical reflector for systems requiring process heat and make possible substantial utilization of solar energy and considerable savings relative to fossil energy in the sunny countries of the world.

keywords: Spherical reflector, Circle of least diffusion, Cylindrical receiver, Optical characteristics, Thermal characteristics, Runge-Kutta method;

1. Introduction

All systems, which harness and use the sun's energy as heat, are called solar thermal systems. These include solar water heaters, solar air heaters, and solar stills for distilling water, crop driers, solar space heat systems and water desalination systems. Temperatures far above those attainable by flat-plat

Nomenclature

A_r: absorber area (m^2)

* Corresponding author. Tel.: +233556879994; fax: +23341421213.
E-mail address: Khaled_mahdi@yahoo.fr.

A_a : aperture area (m^2)

A_r : receiver area (m^2)

S : Mirror area (m^2)

D: diameter of spherical reflector (m)

D_a : diameter of receiver absorber (m)

R : Radius of spherical reflector (m)

C : Collector concentration ratio =$\left[\frac{A_a}{A_r}\right]$; factor

Cp: Parabolic concentrating

Cs : Spherical concentrating

T_r: Receiver temperature ($°C$)

T_∞: Ambient temperature ($°C$)

G_h : Global horizontal radiation (W/m^2)

I_N : Incident normal radiation (W/m^2)

h : solar altitude

Greek symbols

α : Absorbance

θ : Angle rim of mirror

θ_m: Maximal angle rim of mirror

δ_{lon}: Longitudinal aberration

δ_{tran} : Transversal aberration

ρ_m: mirror reflectance

η_o: Optical efficiency

Δt : Step time (s)

Δx: step space (m)

α_w Thermal diffusivity of water (m^2/s)

λ_w : Thermal conductivity of water (W/mK)

ρ_w: Density of water (kg/m^3)

c_w : Specific heat of water (J/kgK)

λ_s: Thermal conductivity of steel (W/mK)

c_s : Specific heat of steel (J/kgK)

1: first experience

2: second experience

Collectors can be reached if a large amount of solar radiation is concentrated on a relatively small collection area. This is done by interposing an optical device between the source of radiation and the

energy absorbing surface. Concentrating collectors exhibit certain advantages as compared with the conventional flat-plate type, Planar and non-concentrating type which provides concentration ratios of up to four and are of the flat plate type. Line focusing type produces a high density of radiation on a line at the focus. Cylindrical parabolic concentrators are of this type and they could produce concentration ratios up to ten. Point focusing types generally produce much higher density of radiation in the vicinity of this point. A paraboloïdal reflector is example of point focus concentrators. Spherical solar collector is an attractive method to concentrate direct beam radiation which converts it to thermal energy in a useful form for electrical power generation [1]. Solar thermal power plants with concentration technologies are important candidates for providing the bulk solar electricity needed within the next few decades. Four concentrating solar power technologies are developed: parabolic trough collectors, linear Fresnel reflector systems, power towers or central receiver systems and dish engine systems [2]. The design of a receiver of solar heat in the operating temperature range (150°C-500°C) requires the study and the optimization in order to characteristic the receiver absorber surface using the heat balance. The optical properties of absorbing receiver are important for characterizing the type of solar radiation concentrator, the geometric concentration ratio defined as the ratio of the apparent surface of the mirror and apparent surface receptor absorber to home mirror is used, for a given operating temperature. The thermal efficiency increases not practically beyond a certain value of the concentration ratio and this is likely to facilitate the recovery of heat and limit technological difficulties when performing the mirror concentrator. The choice of the latter requires knowing the values of concentration ratio as a function of tolerance of various kinds like, that induced by the automatic tracking of the sun. It is for this reason that we apply such a calculation mirror ball from a cylindrical receiver two different positions are proposed in our study, the first dealing with the heat exchange surface side wall and the second heat exchange surface receptor at the lower diffusion circle. The spherical concentration presented a second type of compound curvature collector using spherical geometry instead of parabolic geometry. (Fig. 1) shows ray traces in a plane of symmetry for normal incidence (tow axis tracking) on a spherical concentrator. The parallel rays in this case are focused along a line which extends from the surface of the mirror to a distance of R_0 / 2 from this surface, as in the case of other compound curvature mirrors. It is also clear that rays intercepted near the cylindrical receiver base intercept the absorber at very large incident angles. Therefore, an absorber envelope with very low reflectance or no envelope at all is used to avoid severe penalties to the optical efficiency, in our research work, the second choice is used.

2. Mathematical model

2.1. Optical model and analysis

The optical scheme of a spherical concentrator in the axial section coincides with the scheme of circular cylindrical reflector. An arbitrary point of the spherical concentrator the radius R that is defined by the angular coordinate θ reflects the incident ray that is parallel to the optical axis at the angle $\pi/2 - 2\theta$ to the abscissa axis (Fig. 1).

The equation of the reflected ray has the form [3]:

$$x = \frac{R}{2}\left[1 - \left(\frac{r}{R}\right)^{2/3}\right]^{1/2}\left[1 + \left(\frac{D_r}{2R}\right)\left(\frac{R}{r} - \frac{2r}{R}\right)\right] \quad (1)$$

The family of the reflected rays with the parameter θ forms the envelope of these rays, which is described by the parametric equations [3]:

$$x = \frac{R}{2}\cos\theta\,[1 + 2sin^2\theta] \quad (2)$$

$$r = Rsin^3\theta \quad (3)$$

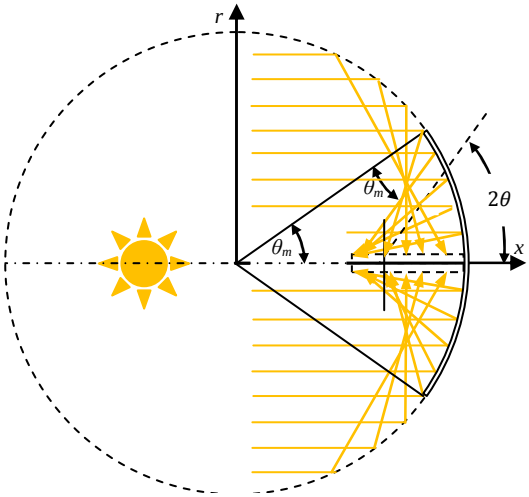

Fig.1 Optical scheme of spherical concentrator.

When the incident rays are inclined on the axis of the mirror, the situation is much more complicated. The caustic is no longer a surface of revolution (see **Fig**.2 and 3). For a mirror of small aperture, the light focuses on two short line segments orthogonal, tangential focal and sagittal focal between which is a circle of least confusion. The influence of the rim angle on the overall system efficiency will be shown later. The advantages of using rim angles less than 90° are greater mirror utilization and a reduction in construction costs due to fewer mirrors.

$$\frac{S}{A_a} = \frac{2(1-\cos\theta)}{sin^2\theta} \tag{4}$$

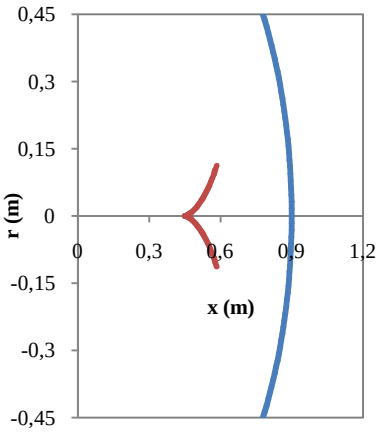

Fig 2. Caustic for spherical reflector for rim angle $\theta_m = 30°$

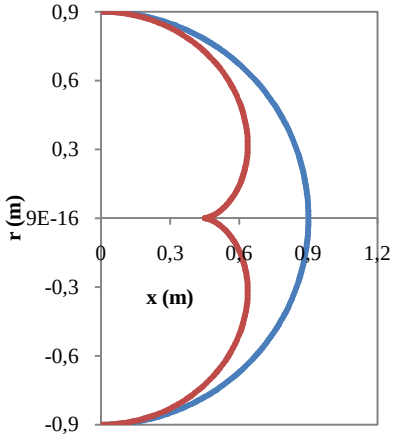

Fig 3. Caustic for spherical reflector for rim angle $\theta_m = 90°$

The mirror area of a hemispherical reflector is twice the aperture area. Whereas, it approaches the aperture area as the rim angle approaches zero.

The concentration of the parabolic dish is greater than the spherical concentration. the concentration of a parabolic dish increases with the aperture angle of the dish, on the other hand the spherical dish is better in the aperture angle of 22° where the concentration is maximum [2,7].

The figure 5 shows the study of the ratio (*Cp/Cs*), *Cp* geometric concentration of parabolic dish with an aperture of 30°, on *Cs* geometric concentration of spherical dish, in relation to the aperture angle θ for large values of this angle. The spherical mirror is preferable because of its simplicity of realization.

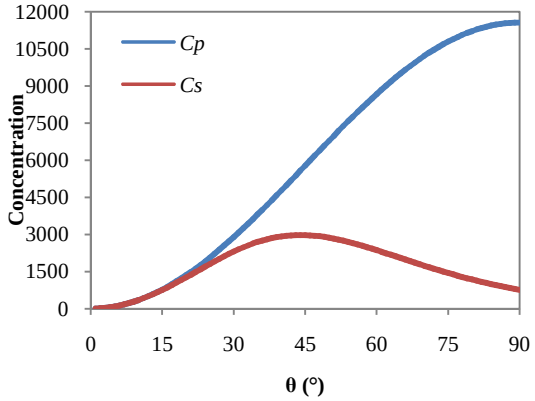

Fig. 4 Variation in the concentration ratio between spherical and parabolic concentrator

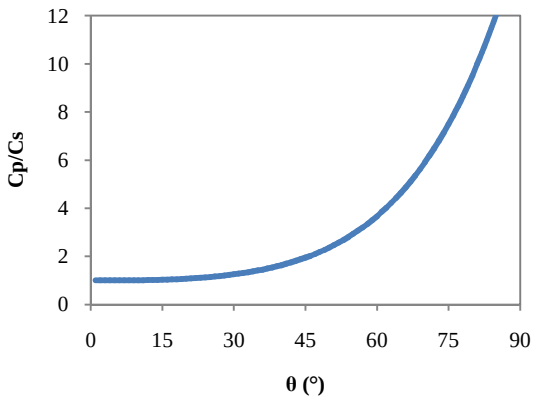

Fig.5 comparison between the spherical concentrator and parabolic concentrator

The concentration of the energy at an arbitrary point of the focal plane is determined by the equation of the energy balance between the annular reflector and receiver elements, including this point,

$$2\pi\rho_m I_N r dr = \pi D_r Q_c(x) dx \tag{5}$$

Finally Heat flux distribution is given by:

$$Q_c(x) = \frac{2\rho_m I_N r}{D_r}\frac{dr}{dx} \qquad , 0.45 < x < 0.9 \tag{6}$$

The relatively large cylindrical receiver required in the Spherical reflector system may be partially offset in some applications by the non uniform energy distribution along the "line" focus. For a constant diameter, circular cylinder is used as the absorber with a reflector having a rim angle varying between 0° and 90°, the ratio of the local heat flux on the receiver $Q_c(x)$ to the average I_N when the sun's rays are normal to the aperture by approximate solution [5] is :

$$Q_c(x) = \frac{\rho_m I_N}{2D_r}\frac{1}{x^3} \tag{7}$$

For cylindrical envelope the incident angle i is given by the following formula:

$$i = \frac{\pi}{2} - 2sin^{-1}\left(\frac{r}{R}\right) \tag{8}$$

and

$$P_{in1}(x) = A_a \eta_0 Q_c(x) cosi \tag{9}$$

Where:

$$\eta_0 = \rho\gamma\alpha \qquad (10)$$

$Q_r(x)$ is the cylindrical receiver incident flux by spherical reflector, and η_0 is the optical efficiency is the product of $\rho, \alpha \; and \; \tau$ .A spectral reflectance ρ is between 0. 85 and 0.9 is typical for high quality mirrors. The solar absorptance α of a selective surface characteristically lies between 0.85 and 0.95.

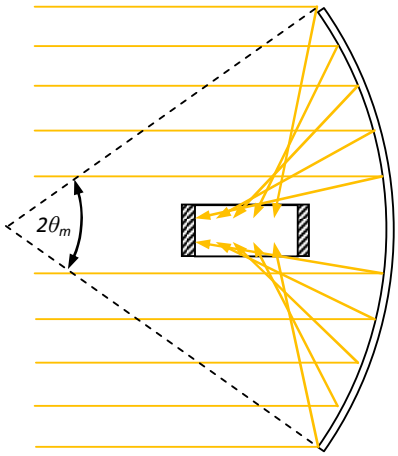

Fig.6 heat exchange with the side wall of a cylindrical receiver (model 1)

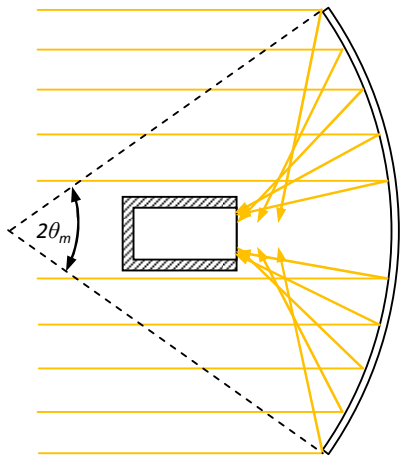

Fig. 7 heat exchange with the base of a cylindrical receiver (model 2)

The use of a cover plate seems illogical due to the high reflective loss for rays at large angles of incidence, γ is the intercept factor, and i is the angle of incidence with optical axis.
The **Fig.6** and **Fig.7** show the different positions for receiver, the first model represents heat exchange with the side wall of a cylindrical receiver, and the second one represents heat exchange with the base of a cylindrical receiver.

As shown in **Fig.8**, the cylindrical receiver surface flux increases with non-uniform energy distribution along the "line" focus, a line which extends from the surface of the mirror to a distance of R/2 from this surface. Hence, an absorber which is to intercept all of the specularly reflected energy from such a spherical mirror must have a length of approximately R/2. We notice that on the abscissa of line focus the least diffusion circle incident flux is maximal.

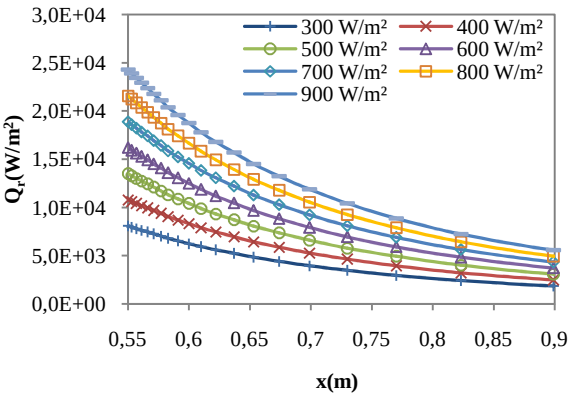

Fig.8 The Influence of line focus on cylindrical receiver flux for different incidents solar radiation (model 1)

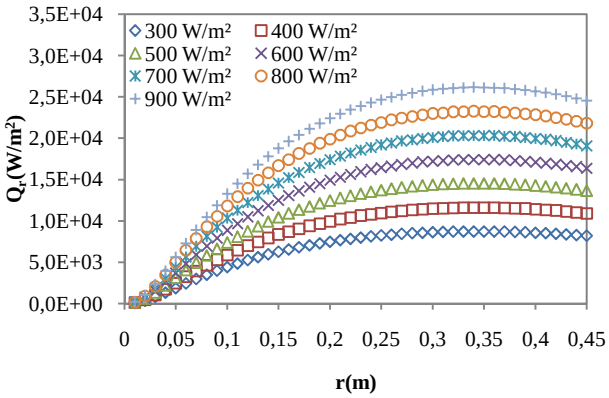

Fig. 9 The Influence of ray on cylindrical receiver temperature for different incidents solar radiation (model 2)

Fig.9 shows the temperature distribution in relation to the line focus, so it seems it has the same appearance as **Fig.8.** The cylindrical receiver temperature distribution is influenced by the different solar incident radiation.

2.2 Thermal model and analysis

In this first effort to describe the solar spherical collector, we selected the simplest thermodynamic model of the system (1st thermodynamic law). The model comes from an energy balance done on the thermodynamic system we defined (Fig. 10).

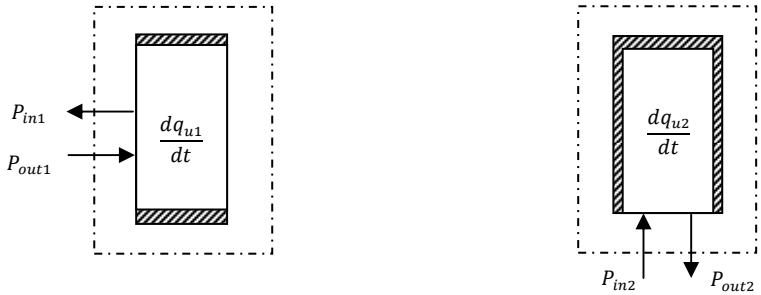

Fig.10 Boundary of the thermodynamic system, 1 index for model one, 2 index for model 2

The thermodynamic system is closed system composed of the cylindrical receiver made of steel and water that gives form to the absorber. Under these assumptions, the general energy balance is given by

$$P_u = P_{in} - P_{out} \tag{11}$$

Where P_u is the instantaneous change in internal energy of the system, , $P_{in}$is the energy by unit time that arrives at the boundary of the system and P_{out} out is the loss of energy by unit time that leave the boundary of the system.
The incoming energy is given by the only energy source, the solar radiation concentrated by the spherical reflector. The amount of energy the concentrator can provide the system is

$$P_{in1} = C\alpha\rho A_a I_N \tag{12}$$

$$P_{in2} = \frac{\rho_m I_N}{2D_r}\frac{1}{x^3}A_a\eta_0 cosi \tag{13}$$

here C is the geometric concentration parameter for the spherical reflector, which is dimensionless and defined as the surface area of the concentrator over the surface area of the concentrated image, α is the optical absorptance of the surface of cylindrical receiver (which was painted black [10]), which is also dimensionless, ρ is the optical reflectance of spherical reflector, A_s(m^2) is the surface area that is used up by the image that the mirror over of the cylindrical receiver for first experience and for second experience over lateral wall of cylindrical receiver, finally I_N (W/m^2) is the instantaneous irradiance, which can be measured using a horizontal global by Pyranometer from station meteorological of CDER.
The heat loss P_{out} from the receiver with the simplifying assumptions the losses of the system are given by:

$$P_{out} = hA_r(T_r - T_a) + \sigma\varepsilon A_r(T_r^4 - T_s^4) \tag{14}$$

where h (W/m^2 K) [12] is the convective heat transfer coefficient between the coffee maker and the surroundings, A_r (m^2) is the total external area of the coffee maker, T_r (°C) is the instantaneous temperature of the thermodynamic system, T_a (°C) is the temperature of the environment surrounding the thermodynamic system, ϵ is the emissivity of the aluminum of the coffee maker, σ is the Stefan-

Boltzmann constant (5.67x 10^{-8} W/m^2 K^4) , and T_s (°C) is the temperature of the sky which, for practical reasons, we replace with T_a.

The energy losses of the system can be divided into three types, conductive, convective, and radiative. The first type is very small given that the area of steel ring that crosses the boundary of the system is very small, thus we neglect the conductive losses. For the convective losses we use Newton's law of cooling, and for the radiative losses we use the Stefan–Boltzmann equation. Here it is important to stress that the simplest thermodynamic model will consider the system as characterized by only one temperature, neglecting its space variations.
The model takes into account that the change in internal energy presents the evolution of the thermodynamic system. During the experience the mass of water is constant; in this time interval there is an energy influx into the system. The heating of the liquid inside the system is not uniform during this period of experience; the water that is closer to the bottom plaque gets hotter, and less dense, than that at the upper part of the water column. The lower density water is able to go through a phase change process at a lower temperature than the temperature of saturation at ambient pressure. Given all of this we model the change in internal energy as shown in Eq. (4), where $m_w(kg)$ and C_p $(J/kg°C)$ represent the mass and the specific heat at constant pressure, respectively; the subscript Steel indicates steel, and water refers to the water in the system before and up to the time t. Finally dT_r/dt is the rate of change in time of the instantaneous temperature of the system.

$$P_u = (m_s c_s + m_w c_w)\frac{dT_r(t)}{dt} \tag{15}$$

In all cases we model m_w as decreasing linearly. In other words it decreases at a constant rate, from 0.3 kg, which is the amount of water that the cylindrical receiver can hold, to zero kilograms, All this in the time interval of t_1 to t_2.
and solving the set of differential equations by a fourth order Runge-Kutta algorithm. In another paper (Olwi and Khalifa, 1993) [10] they modelled the performance of the solar grill and compared that with experimental results of the tests conducted.

With Equations (2)-(4) substituted into Eq. (1) we can construct a differential equation. We use the measured temperature of the water at time zero as the initial condition. The solution of this equation gives us the instantaneous temperature of the thermodynamic system. Due to the fourth order form of Eq. (3) the resulting differential equation is nonlinear and must be solved by *Runge-Kutta* numerical methods. For this purpose we wrote a program in FORTRAN to solve it [11]. The form of the differential equation that the program solves is shown in Eq. (5).

$$(m_s c_s + m_w c_w)\frac{dT_r(t)}{dt} = C\alpha A_s I_N - hA_c(T_r - T_\infty) - \epsilon\sigma A_c(T_r^4 - T_\infty^4) \tag{16}$$

In order to evaluate the model we use the values presented in **Table 1**. The instantaneous irradiance and the average ambient temperature that was used in the program were measured experimentally. The experimental setup is presented in the next section.

We used a scheme of order one (1) backward to evaluate the time derivative and a centered scheme of order two (2) for the second derivative in space. The temperature with iteration (n+1) is given by:

$$(1 + 2Fo)T_{r,i}^{t+\Delta t} - \beta\left(T_{r,i+1}^{t+\Delta t} + T_{r,i-1}^{t+\Delta t}\right) = T_{r,i}^{t} \tag{17}$$

Where:

$$Fo = \frac{\alpha_f \Delta t}{\Delta x^2} \tag{18}$$

Fo : Fourier number dimensionless
and

$$\alpha_f = \frac{\lambda_f}{\rho_f c_f} \tag{19}$$

α_f is the thermal diffusivity.
i varying from 1 to (n-1), It was found that the unknowns at iteration (n+1) are connected by an implicit method (hence the name of the method), At each iteration the vector of discrete unknowns is determined by solving a linear system in the matrix form, the Gaussian elimination algorithm (based on Gaussian elimination method) is often used. The algorithm is written in FORTRAN.

Table 1. Optical and dimensional characteristics Values used in the theoretical model program.

Item	Symbol/Units	Value
Weather Conditions for Algiers (August 05)		
	T_{min},°C	25
	T_{max},°C	32
The spherical reflector	ρ_m	0.9
	η_{opt}	60%
	Γ	-
Transversal aberration	δ_t, *m*	10.7e-2
Latitudinal aberration	δ_l, *m*	6.18e-2
Aperture Area	A_a, m^2	0.636
Reflector area	*S*, m^2	0,681
Maximal Aperture angle	θ_m, °	30
Focal distance	*f*, *m*	0,45
Reflector area	0.681	m^2
Aperture Area	0.636	m^2
Diameter	D_a, *m*	0.9
Receiver	A_r, m^2	
Receiver aperture	0.0078	m^2
Height	0.2	M
Reflector area	0.681	m^2

The useful heat delivered by a solar collector is equal to the energy absorbed by the heat transfer fluid minus the direct or indirect heat losses from the surface to the surroundings. When neglecting the losses the useful energy collected from a reflector can be obtained from the following formula:

$$P_u = c_p \dot{m} (T_o - T_i) \tag{20}$$

Where P_u is the rate of useful energy delivered by solar dish concentrating collector in W, c_p is specific heat at constant pressure in *J/kg K*, $\dot{m}$ is working fluid mass flow rate in *kg/s*, and T_i, T_o is temperatures of fluid entering and leaving the receiver in °*C*
[9, 40–42].
The spherical concentrator efficiency is also defined as the ratio of the useful energy delivered to the energy incident on the concentrator aperture and a function of water temperatures entering and leaving the receiver and the mass flow rate. Therefore, thermal efficiency can be determined in Eq. (3.14) [43].

$$\text{Thermal efficiency} = \frac{\text{useful energy}}{\text{Heat energy}}$$

Since the aperture area of the solar spherical concentrator A_a is a relevant indicator of the concentrated sun rays, the efficiency equation based on A_a.

$$\eta_{th} = \frac{Q_u}{I_N A_a} = \frac{c_p \dot{m}(T_o - T_i)}{I_N A_a} \quad (21)$$

Where I_N is the beam normal solar radiation in W/m^2 and A_a is aperture area of the solar spherical concentrator in m^2 [9-12].

3. Measurement and analysis

The experiments have been done at center of development of renewable energy-CDER Bouzareah (latitude 36.8° north, longitude 3° East, Altitude 345 m) in summer's season with clear sky conditions. The experiment is made at August 5th, 2008, from 11^{h} to 14^{h}. To determine the space-time evolution of the cylindrical receiver temperature, two thermocouples were installed in equidistant positions along its diameter (see **Fig. 15)**.

3.1 Analysis of experimental data

Data acquisition system makes it possible to follow the evolution of the Temperature given by each thermocouple every five minutes, solar radiation flux and the ambient temperature are given by a weather station installed in situ. The values given by the pyranometer represent the solar flux on horizontal surface (Fig. 12). Figure 13 represents global solar flux variation measured by the meteorological station of the site during the sunny period of the day. The horizontal global solar flux density measured by the pyranometer using an estimated solar altitude h to obtain incident solar flux I_N on the spherical reflector each time during the experiment. The relation is given by the following expression:

$$I_N = \frac{G_h}{\sin(h)} \quad (22)$$

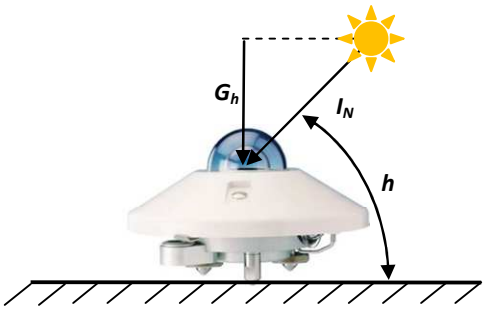

Fig.12 pyranometer

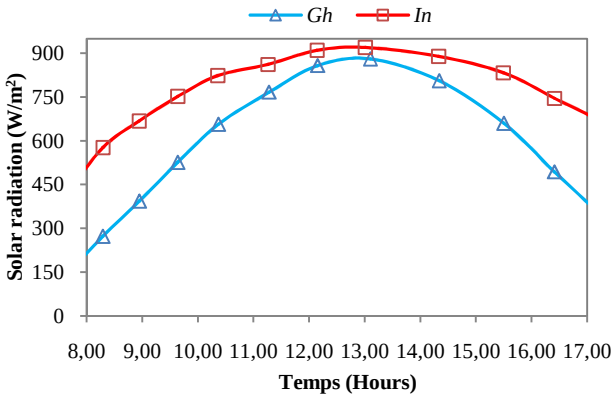

Fig.13 Variation of solar radiation during the test period on 5th, August.

3.2 Experimental study

For our experiment we have dealt only with the second case, the reflector of our experimental device consists of a spherical concentrator of 0.9 meter aperture diameter. Its interior surface is covered with a reflecting layer (mirror) that reflects solar rays on the face of a receiver placed at the focal position. The concentrator is placed on a directional support according to two axes to ensure the follow-up of the sun.
The characteristics of the solar concentrator are shown in **Table 1**.
The reflecting film covering the surface of the spherical reflector is a silver layer with a reflecting coefficient near 0.9.

Fig.14 The solar spherical reflector used in the experiment.

The first experience the receiver has a diameter of 0.1 m, and is covered with a thin coat of black paint having an absorption coefficient near 0.9 and is located in a circle of least confusion (the focal zone) of the concentrator equals to 2.4e-2 m. The receivers' characteristics are shown in **Table 1**. The horizontal global radiation measured during the test and the estimated beam radiation is presented in Fig. 13.

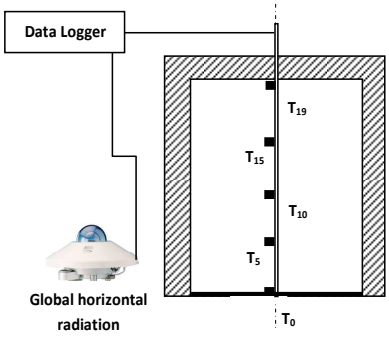

Fig. 15 The cylindrical receiver schematic diagram and data acquisition system

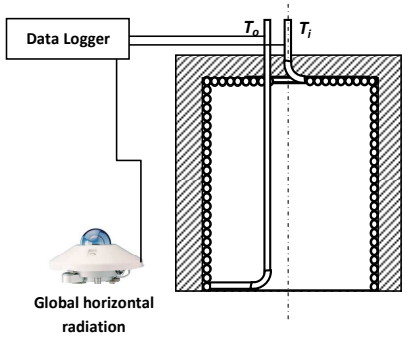

Fig.16 The cylindrical receiver with coil schematic diagram and data acquisition system

4. Results and discussion

Fig.14 shows the correspondence between the points measured by thermocouples and thermal stratification calculated by the model. The thermophysical characteristics of steel are different from those of water, λ_w= 0.6 *W/m K*, λ_s= 48 *W/m* K, c_w(T) = [4180 – 5700] *J/kg K*, c_s = 465 *J/kg K*, and this means that heat transfer by conduction is more significant in the walls of the absorber than in the water inside the receptor. We note that the theoretical curve and the measured levels (thermocouple) have practically the same shape. However, we notice a slight increase at the extremity of the curve which is due to the difference between the physical characteristics of steel (absorber) and those of water such as thermal conductivity and calorie capacity. In fact, the spread of heat by conduction in the absorber (steel) is faster than in water. As a result, the upper part of the absorber becomes a source of heat, hence the increase in temperature.

According to Figure 16, for t = 0 s the difference between the initial tap water temperature and temperature at the coil exit ($T_i = T_o$) is nil. But theoretically the difference is different from zero because the net power which depends on direct solar radiance. We note that the estimation follows the measurement with some fluctuations due to many factors pertaining to the experiment, such as the temporal variation of direct solar illumination because of the passage of clouds.

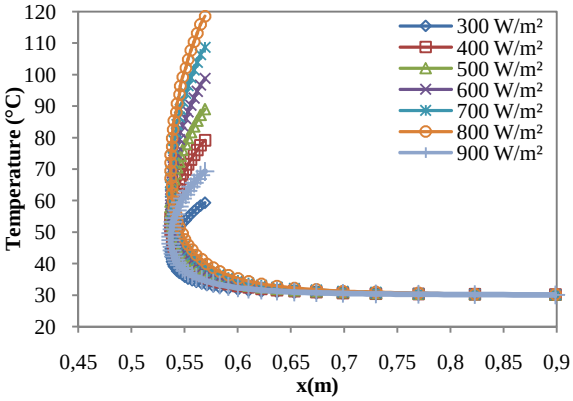

Fig. 17 The temperature distribution in cylindrical receiver

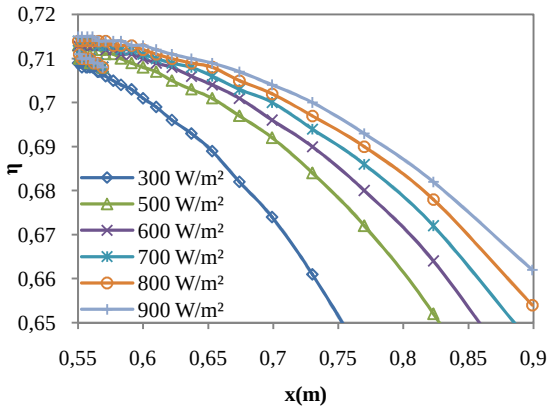

Fig. 18 Thermal efficiency

Thermal efficiencies were calculated using equation (21). Their variations with radius of spherical reflector are shown in Fig. 2 for various solar radiation incidents. As expected, the efficiency is constant for any solar radiation incident up to a radius of spherical reflector about 0.6 m, for which radiation losses start to become significant. At 0.55 m and 900 W/m^2 of solar flux, the efficiency is about 70%, until stagnation temperature point, since radiation losses are negligible and the aperture is big enough to intercept all the power coming from the concentrator.

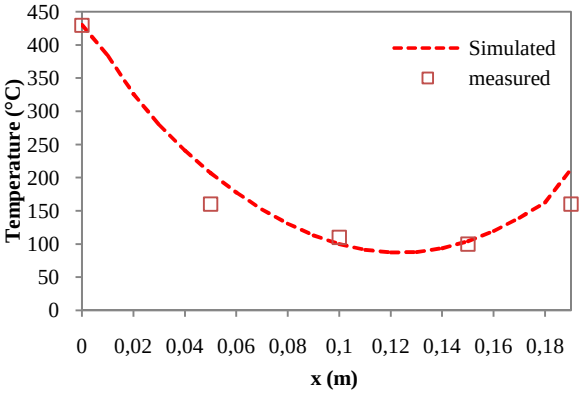

Fig. 17 The cylindrical receiver with coil schematic diagram and data acquisition system

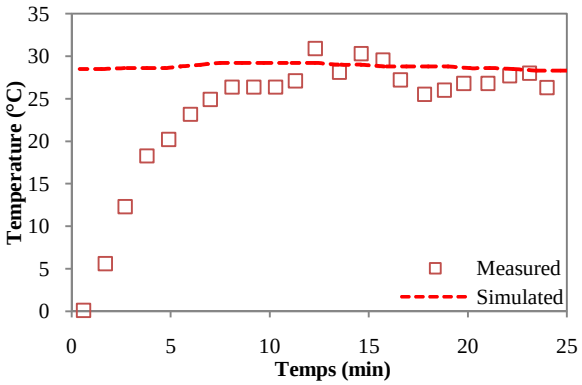

Fig.18 Comparison between the variations in difference regarding measured and estimated Temperatures for ṁ= 0.0007kg/s on August 05.2008

Fig.17 represents temperature evolution of the disk centre. In the experimental conditions mentioned above, the temperature reaches an average value of 270 °C after 23 min which represents the heating time of the receiver. Two comparative experimental studies are made between cylindrical receiver and coil receiver to compare the evolution of vapour production in these two receivers. The first experiment is made on July 26th 2008 and the second experiment on August 5th 2008 for the same period for both, from 11h to 14h. Figure 1 represents the evolution of solar radiation received by the reflector parabolic. As shown in this figure the solar global horizontal radiation can reach in the experiment conditions in average 850 W/m^2 between 11h and 14h.

5. Conclusion

Spherical reflector seems well suited to a number of applications because it is:

- Simple construction,
- Easy to track the sun,
- Low cost,

However, the study highlighted the importance of the cylindrical receiver position, the optimal geometry of the spherical reflector and the cylindrical receiver position for the solar energy concentrated converted to thermal energy are particularly function. Average concentrations of the area may be that of the production of electricity by thermodynamics (steam), but also photocell, by concentrating solar radiation onto solar cells, Production of heat the energy conversion photochemical and photovoltaic.

References

[1] J. A. Duffie and W. A. Beckman, Solar Energy Thermal Processes. Wiley, New York, 1991.

[2] M. Capderou, '*Atlas Solaire de l'Algérie, Tome1, Vol 1 et 2 : Modèles théoriques et Expérimentaux*' Office des Publications Universitaires, Algérie, 1987.

[3] R. Bernard, G. Menguy and M. Schwartz, Le rayonnement solaire conversion thermique et Applications. Edition Tec-Doc, 1980.

[4] C. Perrin de Brichaumbot and C. Vauge, ' Le gisement solaire', Ed. Tech. & Doc., Paris, 1982.

[5] D. Faiman, Solar thermal Collectors. Introduction to solar energy. *Lecture 5 version 3 .1.2003*

[6] O. C. Jorgensen, Collector heat capacity effect on solar system performance, Solar Energy. Vol29. No.2. pp 175-176, Printed in Great Britain. 1982.

[7] O. C. Jorgensen, Collector heat capacity effect on solar system performance, Solar Energy. Vol29. No.2. pp 175-176, Printed in Great Britain. 1982

[8] Efficiency and Renewable Energy, pp. 212 - 216, 2004.

[9] Shuai Y, Xia X-L, Tan H-P. Radiation performance of dish solar concentrator/ cavity receiver ystems. Solar Energy 2008;82(1):13–21.

[10] Kalogirou SA. Solar thermal collectors and applications. Progress in Energy and Combustion Science 2004;30(3):231–95.

[11] Li X, Zhang M, Wang Z, Chang C. The experimental analysis on thermal performance of a solar dish concentrator. In: Proceedings of ISES solar world congress 2007: solar energy and human settlement. 2009. p. 644–50.

[12] Coventry JS. Performance of a concentrating photovoltaic/thermal solar collector. Solar Energy 2005;78:211–22.